

# Microwave Imaging—Location and Shape Reconstruction from Multifrequency Scattering Data

Kamal Belkebir, Ralph E. Kleinman, *Fellow, IEEE*, and Christian Pichot, *Member, IEEE*

**Abstract**—The problem of determining the shape and location of an object embedded in a homogeneous dissipative medium from measurements of the field scattered by the object is considered in this paper. The object is assumed to be an infinite cylinder of known cross section illuminated by a TM plane wave and the scattered field is measured on a line segment perpendicular to the direction of incidence. Measurement data are carried out at three different frequencies for a homogeneous cylinder of known dielectric constant. The location and contour shape are determined using two different reconstruction algorithms, a Newton–Kantorovich (NK) method and the modified gradient (MG) method whose effectiveness and robustness are compared. Both methods are based on domain integral representations of the field in the body. They involve an iterative minimization of the defect between an integral representation of the field measured on the line and the actual measured data. The NK method involves a linearization of the nonlinear relation between the field and the contrast, as well as the solution of a direct scattering problem at each iteration. The MG method seeks the simultaneous reconstruction of the field and the characteristic function of the support of the scatterer without solving a direct problem at each step. Both methods employed the same initial guess and the *a priori* information that the characteristic function is nonnegative.

**Index Terms**—Image reconstruction, inverse problems, iterative methods, microwave imaging, modified gradient, Newton–Kantorovich, nondestructive testing, shape reconstruction, tomography.

## I. INTRODUCTION

THE DEVELOPMENT of reconstruction algorithms for active microwave imaging for applications in nondestructive testing and, more generally, for electromagnetic (EM) and acoustic imaging has gained much interest during the last decade [1]–[22], [32]. There are two general classes of problems which are considered. The first class deals with a global qualitative or quantitative reconstruction of the internal constitutive object [1]–[17] and the second class deals with the reconstruction external boundary and localization [18]–[22].

Manuscript received June 11, 1995; revised December 24, 1996.

K. Belkebir was with the Laboratoire des Signaux et Systèmes (CNRS/ESE), Plateau de Moulon, 91192 Gif-sur-Yvette Cedex, France. He is now with the Electromagnetics Division, Faculty of Electrical Engineering, Eindhoven University of Technology, 5600 MB Eindhoven, the Netherlands.

R. E. Kleinman is with the Center for the Mathematics of Waves, Department of Mathematical Sciences, University of Delaware, Newark, DE 19716 USA.

C. Pichot is with the Laboratoire d'Electronique, Antennes et Télécommunications, Université de Nice-Sophia Antipolis/CNRS, 06560 Valbonne, France.

Publisher Item Identifier S 0018-9480(97)02532-5.

Problems in civil engineering such as detection of voids or mapping of reinforcement in concrete [23], [24] belong to the second class.

Among the various algorithms developed, a first generation of algorithms was based on diffraction tomography [1], [3]–[5], [7] which is a generalization of classical X-ray computer tomography by taking into account diffraction effects. These algorithms provide quasi-real-time approximate reconstructions of the polarization current density distribution (qualitative imaging) and also for a weak scatterer (Born approximation) the complex permittivity distribution (quantitative imaging). The limitations of diffraction tomography stimulated the recent development of iterative methods for complex permittivity reconstruction of highly contrasted objects [2], [8]–[17]. Methods using a pseudoinverse transformation [2], distorted Born [9], dual space [32], or Newton–Kantorovich (NK) [11] algorithms deal with the nonlinearity of the inverse scattering problem and are, therefore, computationally more intense. They are also more sensitive to the ill-posedness. Another method applied to this problem is the modified gradient (MG) method [14], [15], which appears less sensitive to ill-posedness.

EM inverse problems are characterized by their nonlinearity and ill-posedness. The nonlinear nature of EM inverse problems makes the ill-posedness more severe. By ill-posedness (in the sense of Hadamard) it is meant that one of the following conditions is not satisfied: 1) the existence of the solution; 2) the uniqueness of the solution; or the 3) continuity of the inverse mapping. The continuous dependence of the solution on the data is a necessary, but not a sufficient condition for the stability of the solution. While constant progress in computing facilities alleviates the computational burden, the ill-posedness requires good regularization procedures.

For NK and distorted Born iterative methods, one starts from a linearized form of the nonlinear problem and a standard Tikhonov regularization with an identity operator being used. Different strategies were used for finding the regularization parameters [11], [13]. The MG method minimizes a cost functional consisting of two normalized errors in satisfying the field equation and in matching the measured data. The problem is not linearized; however, the two components of the functional are treated separately. No additional regularization procedure was used in the MG method although recent work indicates that the addition of the total variation as a regularizer is very beneficial [25].

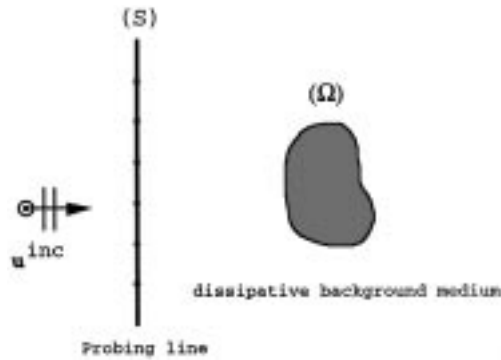


Fig. 1. Cross section of a 2-D homogeneous object embedded in a dissipative background under TM illumination with frequency diversity.

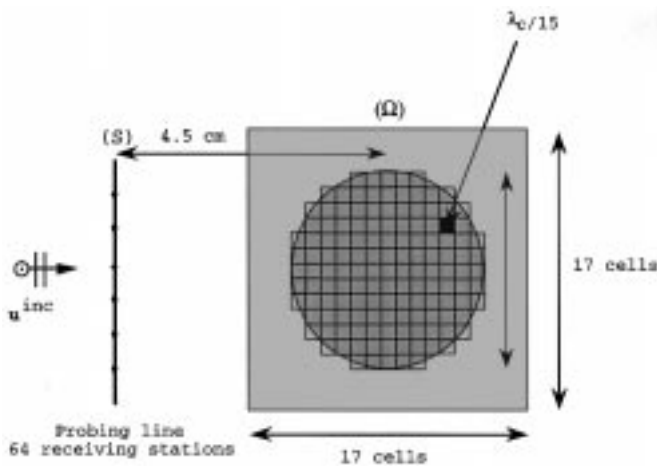


Fig. 2. Numerical modelization of a 10-mm diameter object. The backscattered field is measured over 64 captors.

The problem of determining the shape and location of an object imbedded in a homogeneous dissipative medium from measurements of the field scattered by the object is considered. The object is supposed to be an infinite cylinder of known cross section illuminated by a TM plane wave and the scattered field is measured only on a line segment perpendicular to the direction of incidence rather than at all aspects as in other examples. Measurement data are carried out at three different frequencies for a homogeneous cylinder of known dielectric constant. The multifrequency data is an attempt to compensate for the aspect limitations of the measured data. The location and contour shape are determined using two different reconstruction algorithms, a NK method and the MG method whose effectiveness and robustness are compared. Both methods are based on domain integral representations of the field in the object and discretized using the moment method. The cost functional to be minimized is the normalized error matching the measured scattered data. Different correction directions (standard gradient direction and Polak–Ribière conjugate gradient direction) have been used on the MG method. The initial guess have been determined with a back-propagation scheme using the adjoint operator which provides an estimate of the induced current. As a configuration of practical interest, the reconstruction of a void inside concrete has been studied

## II. CONFIGURATION AND GEOMETRY

The geometry of the problem investigated in this paper is illustrated in Fig. 1. An object region with known dielectric permittivity is embedded in a homogenous medium which can be lossy. The object is known to be contained in, but not necessarily coincide with, a bounded region  $\Omega$ . This object is illuminated by  $J$ -incident plane waves corresponding to  $J$  frequencies. The scattered field is measured on a surface  $S$  situated in the exterior of the object domain  $\Omega$ . In the authors' case, the surface  $S$  is just a line segment perpendicular to the propagation direction of the incident field. The problem is to determine the location and the shape of the object from the multifrequency scattered data assuming that the authors know the texture of the object they are looking for. The inverse problem studied is defined as the following: for given sets of measurements of the scattered field  $f_j$  corresponding to  $J$  frequencies, find the characteristic function  $\chi$  of the object

$$\chi(r) = \begin{cases} 1, & \text{if } r \in \text{Object} \\ 0, & \text{elsewhere.} \end{cases} \quad (1)$$

For inversion, the authors relax the definition of the binary characteristic function  $\chi$  and assume that  $\chi$  can take any real value. Moreover, the authors incorporate *a priori* information such that the characteristic function of the object is nonnegative. Instead of reconstructing  $\chi$ , the authors propose to reconstruct an auxiliary function  $\xi$  such that  $\chi = \xi^2$ , denoted as the object function.

## III. FORWARD PROBLEM

The two-dimensional (2-D) object confined in the  $\Omega$  domain is irradiated by a number of known incident fields  $u_j^{\text{inc}}$ ,  $j = 1, \dots, J$ . For each excitation, the forward scattering problem may be formulated as the domain integral equation

$$u_j^{\text{tot}}(r \in \Omega) = u_j^{\text{inc}}(r) + \int_{\Omega} \xi^2(r') u_j^{\text{tot}}(r') G^{(j)}(|r - r'|) dr' \quad (2)$$

and

$$u_j^{\text{scat}}(r \in S) = u_j^{\text{inc}}(r) + \int_{\Omega} \xi^2(r') u_j^{\text{tot}}(r') G^{(j)}(|r - r'|) dr' \quad (3)$$

where  $G^{(j)}$  is proportional to the free-space Green's function and to the contrast between the object and the embedding medium

$$G^{(j)}(|r - r'|) = \frac{i}{4} (k_{j,\text{obj}} - k_{j,\text{ext}}) H_0^{(1)}(k_{j,\text{ext}}(|r - r'|)). \quad (4)$$

$u_j^{\text{scat}}$  denotes the scattered field measured on the surface  $S$ ,  $u_j^{\text{tot}}$  is the total field inside the test domain  $\Omega$ .  $k_{j,\text{obj}}$  is the wavenumber in the object and  $k_{j,\text{ext}}$  the wavenumber in exterior medium for each frequency  $j$  of the incident wave.

Using the operator notation, (2), (3) can be written in the following compact form:

$$u_j^{\text{tot}} = u_j^{\text{inc}} + G^{(j)} \xi^2 u_j^{\text{tot}} \quad (5)$$

$$u_j^{\text{scat}} = K^{(j)} \xi^2 u_j^{\text{tot}} \quad (6)$$

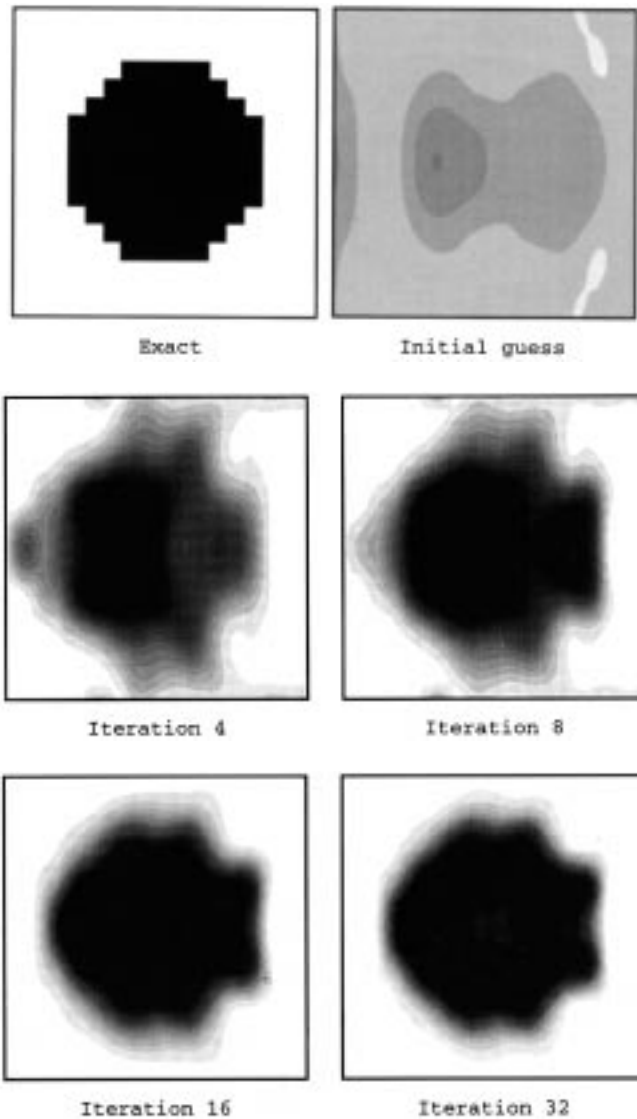


Fig. 3. Reconstruction of the characteristic function  $\chi$  versus iteration with the NK method for noiseless data.

where  $K^{(j)}$  and  $G^{(j)}$  are two integral operators mapping from  $L^2(\Omega)$  into  $L^2(S)$  and  $L^2(\Omega)$  into itself, respectively ( $L^2$  is the square integrable function space). Synthetic data can be generated by solving the direct problem using a moment method [26]–[27] which transforms the integral equations into matrix equations.

#### IV. NEWTON–KANTOROVICH METHOD

In this section the authors describe the NK method [19] which the authors use to solve the  $J$  nonlinear equations relating the data set to the object function

$$f_j = K^{(j)} \xi^2 u_j^{\text{tot}}. \quad (7)$$

The NK method iteratively builds up the solution of (7) by successively solving the direct problem and a local linear inverse problem. At each iteration, an estimate of the object function is given by

$$\xi_n = \xi_{n-1} + \delta\xi \quad (8)$$

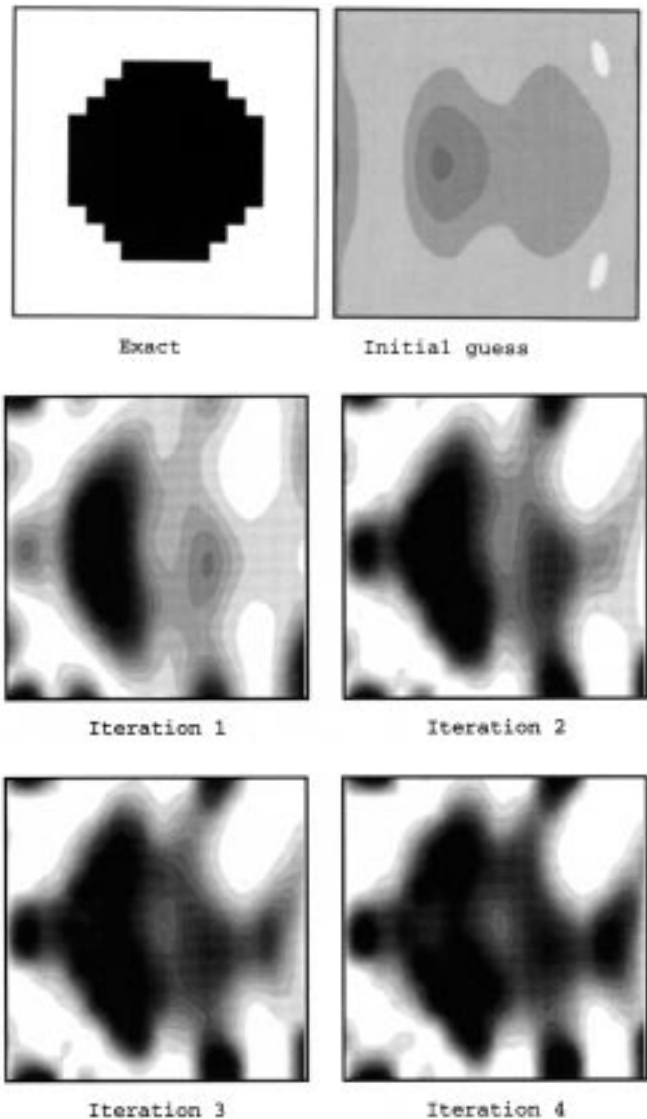


Fig. 4. Reconstruction of the characteristic function  $\chi$  versus iteration with the NK method for noisy data with a SNR of 30%.

where  $\delta\xi$  is an update correction that is obtained by solving in the least squares sense the linearized forward problem

$$\sum_{j=1}^{j=J} D^{(j)} \delta\xi = \sum_{j=1}^{j=J} (f_j - u_{j,n-1}^{\text{scat.}}) \quad (9)$$

where  $D^{(j)}$  is a linearized version of the nonlinear operator relating the scattered field to the object function  $\xi$ .  $u_{j,n-1}^{\text{scat.}}$  is the scattered field calculated through the forward problem solver with a previous estimate of  $\xi$ . Unfortunately, the problem of finding the solution of (9) is ill-posed and needs regularization. The authors use a zeroth-order standard Tikhonov regularization [28]

$$[\bar{D}D + \alpha\mathbf{I}] \delta\xi = \bar{D}(f - u_n^{\text{scat.}}) \quad (10)$$

where  $\alpha$  is the regularization parameter,  $\mathbf{I}$  is the identity matrix, and the overbar means the transposed complex conjugate. The regularization parameter  $\alpha$  is chosen as described in [11].

## V. MODIFIED GRADIENT METHOD

The MG method is iterative as is the NK algorithm, but the approach is very different. Two sequences  $\{u_{j,n}\}$  (total field inside the test domain  $\Omega$ ) and  $\{\xi_n\}$  (object function) are constructed using the following recursive relations:

$$u_{j,n} = u_{j,n-1} + \alpha_{j,n} \nu_{j,n} \quad (11)$$

$$\xi_n = \xi_{n-1} + \beta_n d_n \quad (12)$$

$$r_{j,n} = u_j^{\text{inc}} - u_{j,n} + G^{(j)} \xi^2 u_{j,n} \quad (13)$$

$$\rho_{j,n} = f_j - K^{(j)} \xi^2 u_{j,n} \quad (14)$$

where  $r_{j,n}$  and  $\rho_{j,n}$  are two residual errors. The first one is the residual error with respect to the incident fields in the test domain computed from the coupling equation (6). The second error is the error on the scattered field computed from the observation equation (5). For each step  $n$  the two functions  $\nu_{j,n}$  and  $d_n$  are the update directions for the functions  $\{u_{j,n}\}$  and  $\{\xi_n\}$ , respectively, while the complex numbers  $\alpha_{j,n}$  and the real parameter  $\beta_n$  are weights that are chosen at each step so as to minimize the cost functional  $F_n$ :

$$F_n = \frac{\sum_{j=1}^J \|r_{j,n}\|_{\Omega}^2}{\sum_{j=1}^J \|u_j^{\text{inc}}\|_{\Omega}^2} + \frac{\sum_{j=1}^J \|\rho_{j,n}\|_S^2}{\sum_{j=1}^J \|f_j\|_S^2} \quad (15)$$

where the subscripts  $S$  and  $\Omega$  are included in the norm  $\|\bullet\|$  and later the inner product  $\langle \bullet, \bullet \rangle$  in  $L^2$  to indicate the domain of integration. Once the  $\nu_{j,n}$  and  $d_n$  update directions are found,  $F_n$  is but a nonlinear expression in  $J$  complex variables  $\alpha_{j,n}$  and one real variable  $\beta_n$ . The minimization of  $F_n$  is accomplished using the Polak–Ribière conjugate gradient method [30].

As update directions  $\nu_{j,n}$  and  $d_n$ , the authors take

$$\nu_{j,n} = g'_{j,n} + \gamma_n^{\nu} \nu_{j,n-1} \quad (16)$$

$$d_n = g_n^d + \gamma_n^d d_{n-1} \quad (17)$$

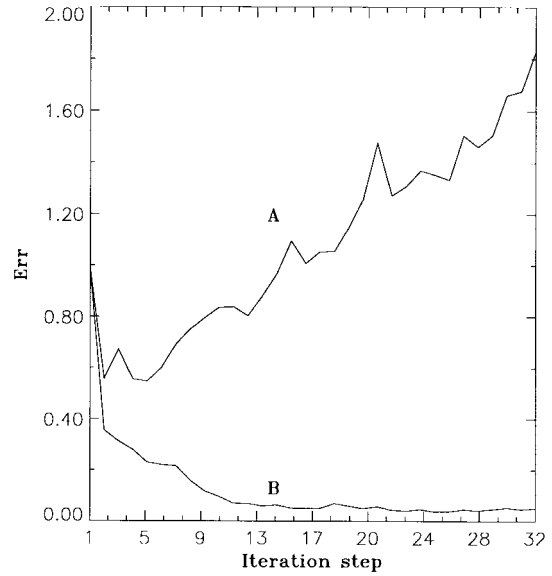
where  $g'_{j,n}$  is the gradient of the cost functional  $F_n$  with respect to the total field assuming that the object function do not changes.  $g_n^d$  is also the gradient of the cost functional  $F_n$  but with respect to the  $\xi$  assuming that the total field do not change.  $\gamma_n^{\nu}$  and  $\gamma_n^d$  are defined as in the Polak–Ribière conjugate-gradient method

$$\gamma_n^{\nu} = \frac{\sum_{j=1}^J \langle g'_{j,n}, g'_{j,n} - g'_{j,n-1} \rangle_{\Omega}}{\sum_{j=1}^J \|g'_{j,n-1}\|_{\Omega}^2} \quad (18)$$

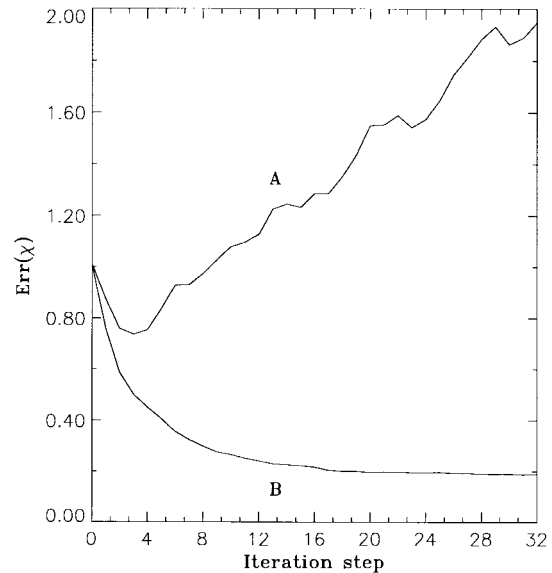
$$\gamma_n^d = \frac{\langle g_n^d, g_n^d - g_{n-1}^d \rangle_{\Omega}}{\|g_{n-1}^d\|_{\Omega}^2} \quad (19)$$

## VI. INITIAL GUESS

In both iterative methods, the authors cannot start from a zero estimate for the object function; instead, a more careful choice must be made. The contrast gradient  $g^d$  in the MG method vanishes for zero values of  $\xi_{n-1}$  and in the NK method the operator  $D$  is null for zero values of  $\xi_{n-1}$ . The authors use the initial guess as in [15] which is determined in three steps.



(a)



(b)

Fig. 5. Evolution of: (a) Normalized rms (NRMS) error of the characteristic function  $\chi$  versus iteration. Curve A: for noisy data with a SNR of 30%. Curve B: for noiseless data. (b) NRMS error of the scattered field versus iteration. Curve A: for noisy data with a SNR of 30%. Curve B: for noiseless data.

*First Step:* The authors calculate an estimate of the sources induced in the object  $\eta_j = \xi^2 u_j^{\text{tot}}$  from the first-kind Fredholm integral equation relating the sources in  $\Omega$  with the scattered field measurements  $f_j$  on the surface  $S$

$$K^{(j)}(\eta_j) = f_j. \quad (20)$$

The estimate  $\eta_{j,0}$  is obtained by back propagating the measured data into the domain by the equation

$$\eta_{j,0} = \gamma \bar{K}^{(j)} f_j. \quad (21)$$

Where  $\bar{K}$  is the adjoint of the operator  $K$  and maps  $L^2(S)$  into  $L^2(\Omega)$ . The complex parameter  $\gamma$  is chosen to minimize the cost function  $\mathcal{F}(\gamma)$  defined as the quadratic error in the

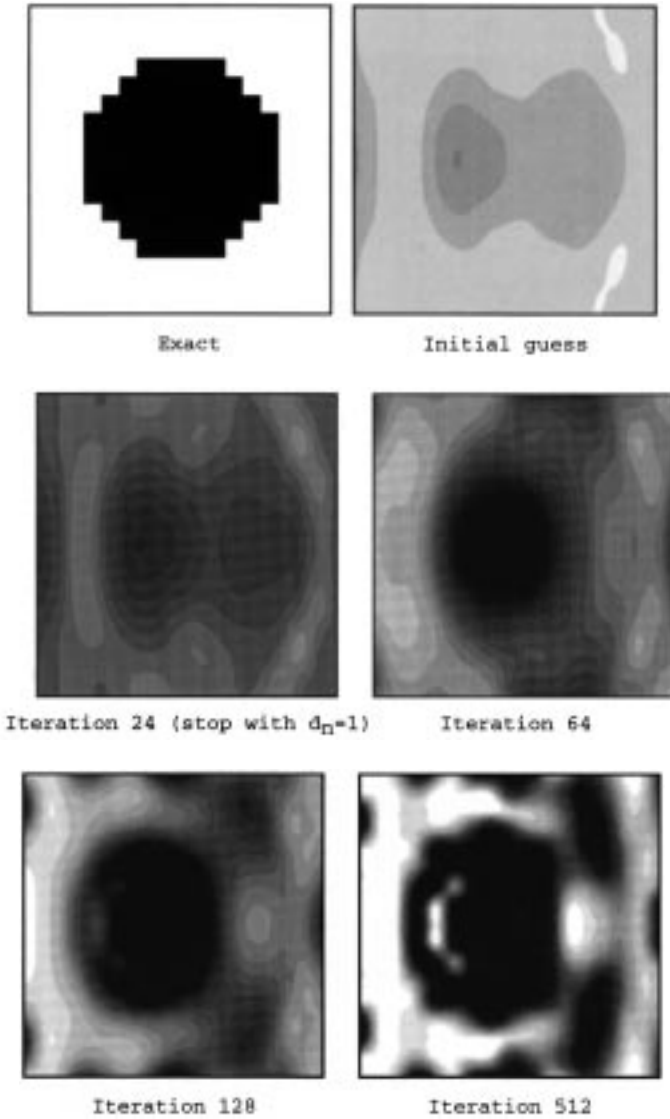


Fig. 6 Reconstruction of the characteristic function  $\chi$  versus iteration with the MG method for noiseless data. Update directions  $d_n$  and  $\nu_n$  were taken to be zero at the points of the test domain where the characteristic  $\chi$  exceeds the limit value.

scattered field

$$\mathcal{F}(\gamma) = \sum_{j=1}^J \|f_j - K^{(j)}\eta_{j,0}\|_S^2 = \sum_{j=1}^J \|f_j - \gamma K^{(j)}\bar{K}^{(j)}f_j\|_S^2. \quad (22)$$

The minimum of  $\mathcal{F}(\gamma)$  with respect to  $\gamma$  is given by

$$\gamma = \frac{\sum_{j=1}^J \langle f_j, K^{(j)}\bar{K}^{(j)}f_j \rangle_S}{\sum_{j=1}^J \|K^{(j)}\bar{K}^{(j)}\|_S^2}. \quad (23)$$

*Second Step:* The authors calculate the initial total field inside the test domain, which is not needed for the NK method by applying the coupling equation (6)

$$u_{j,0}^{\text{tot}} = u_j^{\text{inc}} + G^{(j)}\eta_{j,0}. \quad (24)$$

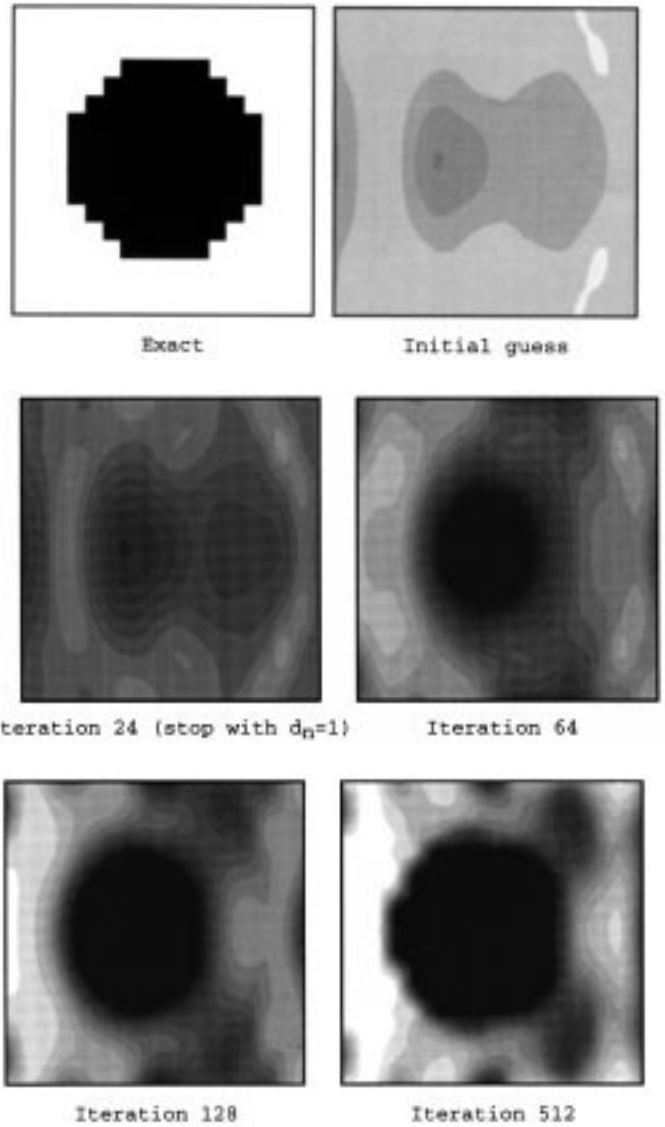


Fig. 7 Reconstruction of the characteristic function  $\chi$  versus iteration with the MG method for noiseless data. Only the update direction relative to  $\chi$  ( $d_n$ ) is taken to be zero.

*Third Step:* The initial guess  $\xi_0$  follows from a minimization procedure of the error in the constitutive relationship  $\eta_j = \xi^2 u_{j,0}^{\text{tot}}$ . For the initial estimate this relation is rewritten as

$$\text{Re}[\eta_{j,0}(r)\bar{u}_{j,0}^{\text{tot}}(r)] = \xi_0^2(r)|\bar{u}_{j,0}^{\text{tot}}(r)|^2. \quad (25)$$

Once the initial estimates for the sources  $\eta_{j,0}$  and the total field  $u_{j,0}$  have been determined, the initial guess for the object function  $\xi_0$  is then determined by minimizing the following cost function:

$$\mathcal{F}(\xi_0(r)) = \sum_{j=1}^J \left( \frac{\text{Re}[\eta_{j,0}(r)\bar{u}_{j,0}^{\text{tot}}(r)]}{\xi_0(r)|u_{j,0}^{\text{tot}}(r)|} - \xi_0(r)|u_{j,0}^{\text{tot}}(r)| \right)^2. \quad (26)$$

Minimization of this expression yields

$$\xi_0^2(r) = \sqrt{\frac{\sum_{j=1}^J \frac{\text{Re}[\eta_{j,0}(r)\bar{u}_{j,0}^{\text{tot}}(r)]^2}{|u_{j,0}^{\text{tot}}(r)|^2}}{\sum_{j=1}^J |u_{j,0}^{\text{tot}}(r)|^2}}. \quad (27)$$

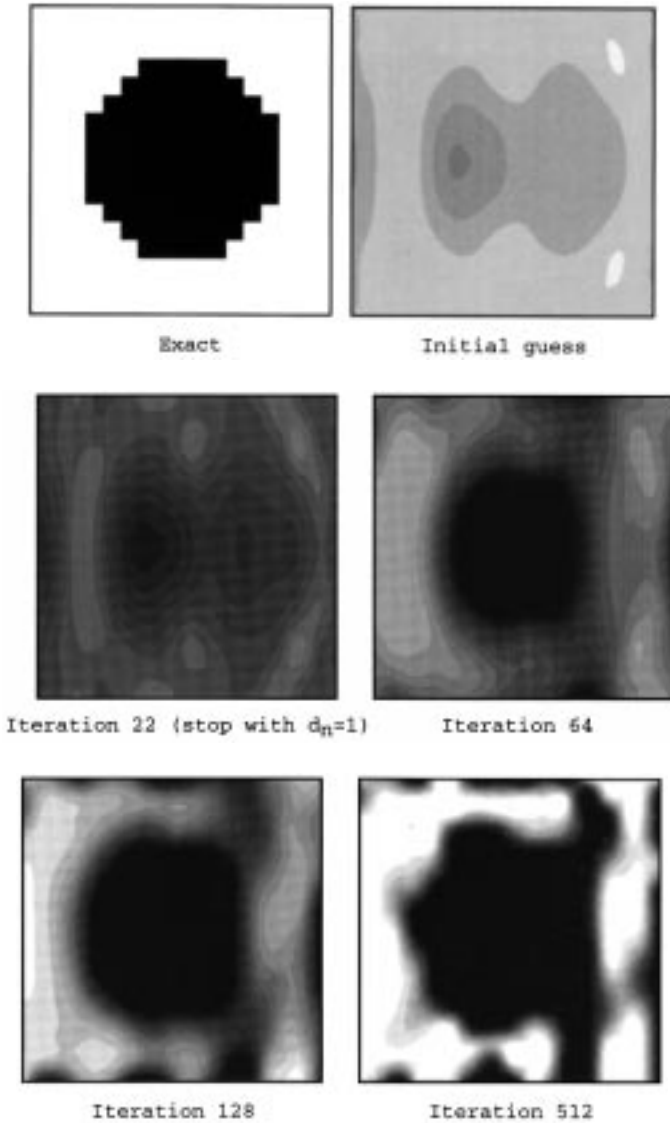
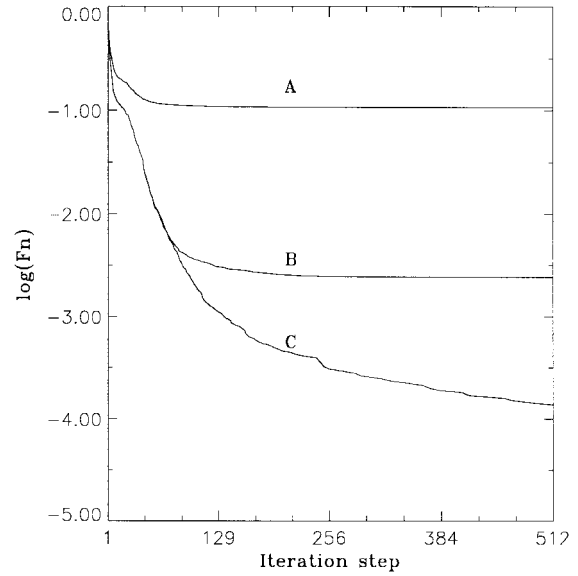


Fig. 8. Reconstruction of the characteristic function  $\chi$  versus iteration with the MG method noisy data with a SNR of 30%. Only the update direction relative to  $\chi(d_n)$  is taken to be zero.

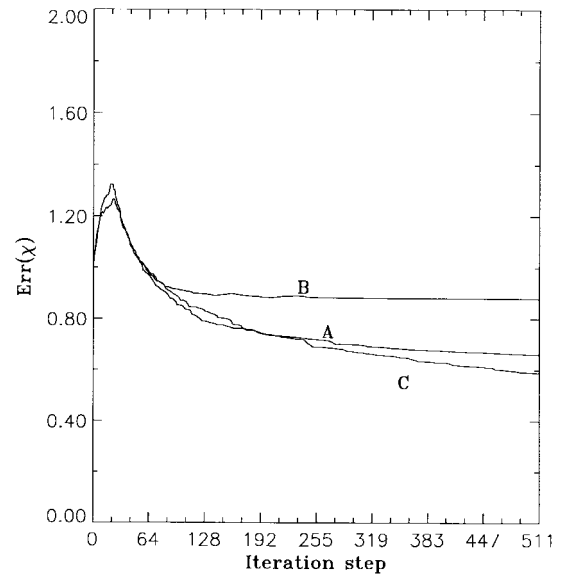
For the NK method, the authors use the initial estimate of the object function  $\xi_0$  defined in (27) and for the MG scheme the authors add the estimate of the total field  $u_{j,0}$  inside the test domain  $\Omega$  given in (24).

## VII. NUMERICAL RESULTS

In this section, the authors present the results of different numerical examples. In these examples, the test domain is taken to be square and subdivided into  $17 \times 17$  subsquares of equal sizes. The object to reconstruct is a void (Fig. 2) embedded in a dissipative medium characterized by a relative dielectric permittivity  $\epsilon_r = 5.0$  and a conductivity  $\sigma = 0.12$  S/m. These values correspond to a relatively dry concrete medium [23]. The authors utilize three frequencies (7, 10, and 13 GHz) and the reflected scattered field is taken over 64 points along a segment line of 32 cm perpendicular to the propagation vector. For the central frequency 10 GHz, the wavelength  $\lambda_c$  in the background medium is about 1 cm. The



(a)



(b)

Fig. 9. (a) Evolution of the cost functional  $F_n$  versus iteration. (b) Characteristic function  $\chi$  versus iteration. Curves A, B, and C correspond, respectively, to noisy data with a SNR of 30% noiseless data and to the case depicted in Fig. 7.

object diameter is 1 cm embedded at a depth of about 4.5 cm (from the interface to the object center).

The reconstruction of the object characteristic function is carried out by NK and MG iterative methods. The initial guess is based on the backpropagation scheme explained in Section VI.

Figs. 3 and 4 show the reconstruction of the characteristic function  $\chi = \xi^2$  with the NK method. Fig. 3 is obtained from noiseless synthetic data and Fig. 4 from noisy data and a signal-to noise ratio (SNR) of 30%. The binary feature [29] of the problem is not taken into account here. That is, even though  $\xi^2$  is known to take only the values zero or one, this information was not integrated in the algorithm and was allowed to vary continuously or, in the discretized case,

to take on any constant value in each subsquare with one important restriction that values exceeding unity were forced to remain at one. The authors note that, in the case of noiseless data, the reconstruction give a satisfactory result after very few iterations, particularly for the illuminated side. But the NK method diverges with 30% noisy data. This is clearly shown in Fig. 5(a) and (b) with the normalized normalized root mean square (NRMS) error of the scattered field and of the characteristic function  $\chi$ , respectively, versus the number of iterations for noisy (curve A) and noiseless (curve B) data.

Figs. 6–8 show the reconstructions of the characteristic function  $\chi = \xi^2$  with the MG method. The initial guess is based on the backpropagation scheme, as is the NK method. The iterative procedure begins with a sequence of update directions ( $d_n = 1$  and  $\nu_n$  is taken to be the conjugate gradient direction) [15] and retained until the normalized change in the field  $\varepsilon_n$

$$\varepsilon_n = \frac{\sum_{i=1}^I \|u_{i,n}^t - u_{i,n-1}^t\|_{\Omega}^2}{\sum_{i=1}^I \|u_{i,n-1}^t\|_{\Omega}^2} \quad (28)$$

is smaller than  $\varepsilon$  (taken to be  $10^{-2}$ ), then  $d_n$  is taken to be the conjugate gradient direction. As in the NK method, values of  $\chi$  exceeding unity were forced to remain at one. For Fig. 6, the update directions  $d_n$  and  $\nu_n$  were taken to be zero at the points of the test domain where the characteristic  $\chi$  exceeds the limit value. For Fig. 7, only the update direction relative to  $\chi$  ( $d_n$ ) is taken to be zero. A better reconstruction is observed in the case of Fig. 7. Fig. 8 shows the reconstruction with noisy data and a SNR of 30%. Fig. 9(a) and (b) shows, respectively, the cost functional  $F_n$  and the normalized rms error of the characteristic function  $\chi$ . Curve A in each figure corresponds to the noisy data whose reconstruction is shown in Fig. 8, curve B corresponds to the noiseless data whose reconstruction was carried out with update directions as used for the reconstruction in Fig. 6, while curve C corresponds to the case depicted in Fig. 7.

### VIII. CONCLUSION

Two iterative methods (one based on NK and the other on MG) have been used for determining the shape and location of a cylindrical object embedded in a dissipative background medium under TM illumination at three different frequencies. Measurements of the scattered field were obtained along a line segment. Noiseless and noisy synthetic data were used in order to investigate the performance of the two reconstruction algorithms. Both methods gave satisfactory results for noiseless data. However, for noisy data with a SNR of 30%, the NK method diverged while the MG method succeeded in reconstructing an image with a noisy distortion roughly equivalent to the magnitude of the noise.

### REFERENCES

- [1] A. J. Devaney, "Geophysical diffraction tomography," *IEEE Trans. Geosci. Remote Sensing*, vol. GE-22, pp. 3–13, Jan. 1984.
- [2] M. M. Ney, A. M. Smith, and S. S. Stuchly, "A solution of electromagnetic imaging using pseudoinverse transformation," *IEEE Trans. Med. Imaging*, vol. MI-3, pp. 155–162, Dec. 1984.
- [3] Ch. Pichot, L. Jofre, G. Peronnet, and J. Ch. Bolomey, "Active microwave imaging of inhomogeneous bodies," *IEEE Trans. Antennas Propagat.*, vol. AP-33, pp. 416–425, Apr. 1985.
- [4] L. Chommeloux, Ch. Pichot, and J. Ch. Bolomey, "Electromagnetic modeling for microwave imaging of cylindrical buried inhomogeneities," *IEEE Trans. Microwave Theory Tech.*, vol. MTT-34, pp. 1064–1076, Oct. 1986.
- [5] W. Tabbara, B. Duchêne, Ch. Pichot, D. Lesselier, L. Chommeloux, and N. Joachimowicz, "Diffraction tomography: Contribution to the analysis of some applications in microwaves and ultrasonics," *Inverse Problems*, vol. 4, pp. 305–331, Apr. 1988.
- [6] K. J. Langenberg, "Introduction to the special issue on inverse problems," *Wave Motion*, vol. 11, pp. 99–112, 1989.
- [7] J. Ch. Bolomey and Ch. Pichot, "Microwave tomography: From theory to practical imaging systems," *Int. J. Imaging Syst. Technol.*, vol. 2, pp. 144–156, Dec. 1990.
- [8] S. Caorsi, G. L. Gragnani, and M. Pastorino, "Two-dimensional microwave imaging by a numerical inverse scattering solution," *IEEE Trans. Microwave Theory Tech.*, vol. 38, pp. 981–989, Aug. 1990.
- [9] W. C. Chew and Y. M. Wang, "Reconstruction of two-dimensional permittivity distribution using the distorted Born iterative method," *IEEE Trans. Med. Imaging*, vol. 9, pp. 218–225, June 1990.
- [10] L. Garnero, A. Franchois, J. P. Hugonin, Ch. Pichot, and N. Joachimowicz, "Microwave imaging: Complex permittivity reconstruction by simulated annealing," *IEEE Trans. Microwave Theory Tech.*, vol. 39, pp. 1801–1807, Nov. 1991.
- [11] N. Joachimowicz, Ch. Pichot, and J. P. Hugonin, "Inverse scattering: An iterative numerical method for electromagnetic imaging," *IEEE Trans. Antennas Propagat.*, vol. 39, pp. 1742–1751, Dec. 1991.
- [12] Y. M. Wang and W. C. Chew, "Accelerating the iterative inverse scattering algorithms by using the fast recursive aggregate  $T$ -matrix algorithm," *Radio Sci.*, vol. 27, pp. 109–116, Mar.–Apr. 1992.
- [13] A. Franchois and Ch. Pichot, "Generalized cross validation applied to a Newton-type algorithm for microwave tomography," in *Proc. Inverse Problems in Scattering and Imaging*, M. A. Fiddy, Ed., San Diego, CA, July 20–22, 1992, pp. 232–240.
- [14] R. E. Kleinman and P. M. van den Berg, "A modified gradient method for two-dimensional problems in tomography," *J. Comput. Appl. Math.*, vol. 42, pp. 17–35, 1992.
- [15] ———, "An extended range-modified technique for profile inversion," *Radio Sci.*, vol. 28, pp. 877–884, Sept.–Oct. 1993.
- [16] S. Caorsi, G. L. Gragnani, and M. Pastorino, "Numerical electromagnetic inverse-scattering solutions for two-dimensional infinite dielectric cylinders buried in a lossy half-space," *IEEE Trans. Microwave Theory Tech.*, vol. 41, pp. 352–356, Feb. 1993.
- [17] S. Caorsi, G. L. Gragnani, S. Medicina, M. Pastorino, and G. Zunino, "Microwave imaging based on a Markov random field model," *IEEE Trans. Antennas Propagat.*, vol. 42, pp. 293–303, Mar. 1994.
- [18] H.-T. Lin and Y.-W. Kiang, "Microwave imaging for a dielectric cylinder," *IEEE Trans. Microwave Theory Tech.*, vol. 42, pp. 1572–1579, Aug. 1994.
- [19] A. Roger, "A Newton Kantorovich algorithm applied to an electromagnetic inverse problem," *IEEE Trans. Antennas Propagat.*, vol. AP-29, pp. 232–238, Mar. 1981.
- [20] W. C. Chew and G. P. Otto, "Microwave imaging of multiple conducting cylinders using local shape functions," *IEEE Microwave Guided Wave Lett.*, vol. 2, pp. 284–286, July 1992.
- [21] C.-C. Chiu and Y.-W. Kiang, "Microwave imaging of multiple conducting cylinders," *IEEE Trans. Antennas Propagat.*, vol. 40, pp. 933–941, Aug. 1992.
- [22] R. E. Kleinman and P. M. van den Berg, "Two-dimensional location and shape reconstruction," *Radio Sci.*, vol. 29, pp. 1157–1169, July–Aug. 1994.
- [23] Ch. Pichot and P. Trouillet, "Diagnostic of reinforced structures: An active microwave imaging method," *Bridge Evaluation, Repair and Rehabilitation*, A. S. Nowak, Ed., (NATO ASI series). Dordrecht, the Netherlands: Kluwer Academic Publishers, 1991.
- [24] K. Belkebir, Ch. Pichot, J. Ch. Bolomey, P. Berthaud, G. Cottard, X. Derobert, and G. Fauchoux, "Microwave tomography system for reinforced concrete structures," in *24th European Conf. Proc.*, Cannes, France, Sept. 5–8, 1994, vol. 2, pp. 1209–1211.
- [25] P. M. van den Berg and R. E. Kleinman, "A total variation enhanced modified gradient algorithm for profile reconstruction," *Inverse Problems*, vol. 11, pp. L5–L10, June 1995.
- [26] J. H. Richmond, "Scattering by a dielectric cylinder of arbitrary cross section shape," *IEEE Trans. Antennas Propagat.*, vol. AP-13, pp. 334–341, May 1965.

- [27] R. F. Harrington, *Field Computation by Moment Methods*. New York: Macmillan, 1968.
- [28] A. N. Tikhonov and V. Y. Arsenin, *Solution of Ill-Posed Problems*. Washington, D.C.: V. H. Weston, 1977.
- [29] R. E. Kleinman, B. Duchêne, and D. Lesselier, "A nonlinearized iterative approach of the eddy current characterization of voids in a conductive half-space," in *Proc. PIERS*, Dwijk, the Netherlands, July 10–15, 1994, p. 408.
- [30] W. H. Press, B. P. Flannery, S. A. Teukolski, and W. T. Vetterling, "Numerical recipes," *The Art of Scientific Computing*, Cambridge, U.K.: Cambridge Univ. Press, 1986.
- [31] K. Belkebir and R. E. Kleinman, "On the location of an object from spatially limited multifrequency scattering data," in *Proc. PIERS*, Noordwijk, the Netherlands, July 10–15, 1994, p. 520.
- [32] D. Colton and R. Kress, *Inverse Acoustic and Electromagnetic Scattering Theory*. Berlin, Germany: Springer-Verlag, 1992.



**Kamal Belkebir** was born in Algiers, Algeria, in 1966. He received the D.E.A. degree in theoretical physics from the University of Montpellier, France and the Ph.D. degree from the University of Paris XI (Orsay), France in 1990 and 1994, respectively.

He is currently at the University of Eindhoven, the Netherlands working on a Post-Doctoral position. His research interests are forward and inverse scattering techniques in frequency and time domains.



**Ralph E. Kleinman** (M'75–SM'83–F'94) received the B.A. degree from New York University, New York, the M.A. degree from the University of Michigan, Ann Arbor, and the Ph.D. degree from the Technische Hogeschool, Delft, the Netherlands, in 1950, 1951, and 1961, respectively.

He is a Professor of mathematics at the University of Delaware, Newark, DE. He is the author or co-author of over 1000 publications appearing in both books and journals. He is past Chairman of U.S. Commission B, International Scientific Radio Union, Associate Editor of *SIAM J. Applied Mathematics*, and is also Director of the Center for the Mathematics of Waves at the University of Delaware. His research is mainly concerned with mathematical problems associated with the propagation and scattering of acoustic and electromagnetic waves including radar cross-section analysis, integral representations of solutions of the Helmholtz equations, low-frequency perturbation techniques, and inverse scattering and iterative solutions of integral equations.



**Christian Pichot** (M'92) was born in France, in 1951. He received the B.S. and M.S. degrees from the University of Nice, France, the Doctorat de Troisième Cycle and the Doctorat ès Sciences degrees from the University of Paris-XI (Orsay), France, in 1973, 1974, 1977, and 1982, respectively.

In 1978, he joined the Laboratoire des Signaux et Systèmes (CNRS/Ecole Supérieure d'Electricité), Gif-sur-Yvette, France. During the 1989–1990 academic year, he was a Visiting Researcher at the Lawrence Livermore National Laboratory, Livermore, CA. From 1992 to 1995, he was with the Laboratoire d'Informatique, Signaux et Systèmes de Sophia Antipolis (University of Nice-Sophia Antipolis/CNRS), Valbonne, France. He is currently Directeur de Recherche at the Centre National de la Recherche Scientifique (CNRS) in the Laboratoire d'Electronique, Antennes et Télécommunications (University of Nice-Sophia Antipolis/CNRS). His research activities are mainly concerned with direct and inverse scattering of electromagnetic waves in inhomogeneous media and antenna radiation from both numerical and experimental aspects.

Dr. Pichot received, along with his colleagues, the Microwave Prize of the European Microwave Conference in Nuremberg, Germany, in 1983.